3-(7-Dimethylamino)coumarin *N*-phenylsemicarbazones in solution and polymer matrices: Tuning their fluorescence via *para*-phenyl substitution

CrossMark

Marek Cigáň [a,*], Martin Danko [b], Jana Donovalová [a], Jan Gašpar [a], Henrieta Stankovičová [a], Anton Gáplovský [a], Pavol Hrdlovič [b]

[a] *Faculty of Natural Sciences, Institute of Chemistry, Comenius University, Mlynská dolina CH-2, SK-842 15 Bratislava, Slovakia*
[b] *Polymer Institute, Slovak Academy of Sciences, Dúbravská cesta 9, 845 41 Bratislava, Slovakia*

HIGHLIGHTS

- Five new 3-(7-dimethylamino) coumarin *N*-phenylsemicarbazones were synthesized.
- Tuning their fluorescent properties via *para*-phenyl substitution was investigated.
- Solvent polarity (TICT state formation, hydrogen bonds) and polymer matrix effects are discussed.
- Unusual formation of fluorescent H-aggregates in both protic and aprotic polar solvents was observed.
- Several coumarin-semicarbazones qualify as laser dyes in the given medium.

GRAPHICAL ABSTRACT

ARTICLE INFO

ABSTRACT

The photo-physical properties of five new *para*-phenyl substituted derivatives of 3-(7-dimethyl-amino)coumarin *N*-phenylsemicarbazone with various electron-withdrawing substituents R (R=F, Br, CF$_3$, CN or NO$_2$) in the *para*-position on the phenyl ring were investigated in solvents and in polymer matrices. Tuning their fluorescent properties via para-substitution is discussed in terms of Twisted Intra-molecular Charge-Transfer (TICT) state formation, specific solute–solvent interactions (hydrogen bonding), fluorescent H-aggregates formation, and the solvent polarity and polymer matrix effects.

© 2014 Elsevier B.V. All rights reserved.

* Corresponding author. Tel.: +421 2 60296306; fax: +421 2 60296342.
  E-mail addresses: cigan@fns.uniba.sk (M. Cigáň), upoldan@savba.sk (M. Danko), donovalova@fns.uniba.sk (J. Donovalová), gaspar@fns.uniba.sk (J. Gašpar), gaplovsky@fns.uniba.sk (A. Gáplovský), upolhrdl@savba.sk (P. Hrdlovič).

Introduction

The fluorescence of 7-dialkylaminocoumarins is strongly dependent on the polarity, hydrogen bonding ability, pH, the

presence of quest anions, various metal ions, biologically important compounds, chemical warfare agents and the micro-viscosity or rotational hindrance in their local environment [1–26]. Moreover, this class of compounds has received considerable attention due to their ability to lase in the blue–green region [5,17]. The photo-physical properties of these dyes depend on the nature and pattern of substitution of the nitrogen atom of the amino group and appropriate substituents at the 3-, 4-, and 6- positions of the coumarin moiety.

In our recent study [27], the photophysical properties of 7-(dimethylamino)coumarin-3-carbaldehyde and its phenylsemicarbazone were investigated in solvents of various polarity and in differing solvent mixtures. The different fluorescent quantum yield (Φ_F) behaviour of these coumarins in highly polar solvents was discussed in terms of TICT state formation and the specific solute–solvent interactions. 7-(dimethylamino)coumarin-3-carbaldehyde exhibits a strong solvent effect in polar solvents due to the formation of a non-fluorescent TICT state and could prove a useful polarity probe for micro-environments containing hydrogen bonding groups. The high quantum yield in DMSO, DMF and alcohols qualifies coumarinphenylsemicarbazone as a laser dye in the given medium, with k_F higher than k_{nr}. Contrary to previous reports that many H-aggregates are non-fluorescent in nature, the fluorescent H-dimer aggregates' formation of 7-(dimethylamino)coumarin-3-carbaldehyde in alcoholic solutions driven by π^+–π^- interactions was reported there for the first time. Furthermore, the quoted study [17] showed that both coumarins exhibit high Φ_F (with k_F higher than k_{nr}) also in PMMA and PVC polymer matrices.

Herein, the investigation of spectral properties of five new *para*-phenyl substituted derivatives **2**–**6** of coumarinphenylsemicarbazone **1** with various electron-withdrawing substituents in the *para*-position on the phenyl ring (Scheme 1) in solution and polymer matrix is reported. This investigation is necessary for practical application of these new derivatives as sensors or laser dyes. The urea/thiourea moiety plays an important role as anion binding site in various colorimetric or fluorescent chemosensors [28–30]. *Para*-substitution on the phenyl ring in the phenylsemicarbazide chain of coumarin **1** can modify the acidity of hydrogen ions on the urea moiety, and thus affect anion binding and receptor signal intensity. Moreover, tuning of fluorescent properties via *para*-substitution can have a positive influence on the lasing action of these dyes and on their spectral sensitivity to the environmental conditions such as micro-polarity and micro-viscosity. Determined spectral properties of new phenylsemicarbazones **2**–**6** are compared with those for the unsubstituted coumarinphenylsemicarbazone **1** and the parent 7-(dimethylamino)coumarin-3-carbaldehyde.

Experimental and theoretical methods

Synthesis

General

Melting points (uncorrected) were measured on a Kofler hot stage. ¹H- and ¹³C NMR spectra were recorded on Varian Mercury Plus 300 spectrometer operating at 300 MHz for ¹H and 75 MHz for ¹³C in DMSO-d_6 or CDCl$_3$ with TMS as the internal standard. Chemical shifts (δ) are reported in ppm downfield of TMS and coupling constants (J) are expressed in Hertz (Hz). All chemicals and solvents were purchased from major chemical suppliers (Merck, Darmstadt, Germany; Acros Organics, Geel, Belgium; Sigma–Aldrich, St. Louis, MO, USA) in highest grade purity, and all solvents were dried by standard methods and distilled prior to use. Elemental analyses were performed on a Carlo Erba Strumentacione 1106 apparatus.

7-(Dimethylamino)-2-oxo-2*H*-chromene-3-carbaldehyde (Mp 204–205 °C, lit. [1] 205 °C) was prepared in a 3-step reaction,

according to the literature [31]. The structure of the prepared aldehyde was proven by ¹H NMR spectra.

General procedure for the synthesis of 4-(4-substituted-phenyl)semicarbazones

Semicarbazides were prepared according to a modified procedure from the literature [32] (Scheme S1). Phenyl chloroformate (20 mmol) was added dropwise to a mixture of aniline (20 mmol), pyridine (20 mmol) and dry CH$_2$Cl$_2$ (40 mL) in an ice-water bath and stirred at room temperature for 18 h. The mixture was then evaporated under reduced pressure and the residue was poured into saturated NaCl for salting out. The precipitate was filtered, dried, and stirred in hydrazine hydrate (80%, 10 ml) at room temperature for 4 h and then filtered off and recrystallized from ethanol.

General procedure. A solution of phenylsemicarbazide (0.46 mmol) in hot absolute EtOH (3 mL) was added to a solution of carbaldehyde (0.46 mmol; 100 mg) in hot absolute ethanol (5 mL). The reaction mixture was refluxed for 15 min and the desired product precipitated. The precipitate was filtered off and washed with cold ethanol, dried and recrystallized from ethanol, with crystalline solid products obtained in 96–99% yields (Scheme S2).

(*E*)-1-{[(7-dimethylamino)-2-oxo-2*H*-chromen-3-yl]methylidene}-4-phenylsemicarbazone **1**: Synthesis of **1** was published by Donovalová et al. [17].

(*E*)-1-{[(7-dimethylamino)-2-oxo-2*H*-chromen-3-yl]methylidene}-4-(4-fluorophenyl)semicarbazone **2**: Obtained from 4-(4-fluorophenyl)semicarbazide (77 mg) in 98% yield (168 mg), ¹H NMR (DMSO): δ 3.07 (6H, *s*, —N(CH$_3$)$_2$), 6.62 (1H, *d*, *J* = 2.4 Hz, Ar—H), 6.74 (1H, *dd*, *J* = 8.7 Hz, 2.4 Hz, Ar—H), 7.12–7.18 (2H, *m*, Ar—H), 7.52 (1H, *d*, *J* = 9 Hz, Ar—H), 7.64–7.69 (2H, *m*, Ar—H), 7.99 (1H, *s*, H-4), 8.67 (1H, *s*, NH), 8.89 (1H, *s*, NH), 10.85 (1H, *s*, HC=N); ¹³C NMR (DMSO): δ 39.5, 97.1, 108.3, 110.0, 113.3, 114.7, 115.0, 121.6, 121.7, 129.7,134.9, 138.3, 152.9, 153.1, 155.7, 160.6.

Anal. Calcd for C$_{19}$H$_{17}$FN$_4$O$_3$ (368.4) C, 61.95; H, 4.65; F, 5.16; N, 15.21. Found C, 61.92; H, 4.63; F, ndt; N, 15.19.

(*E*)-1-{[(7-dimethylamino)-2-oxo-2*H*-chromen-3-yl]methylidene}-4-(4-bromophenyl)semicarbazone **3**: Obtained from 4-(4-bromophenyl)semicarbazide (111 mg) in 96% yield (191 mg), ¹H NMR (DMSO): δ 3.07 (6H, *s*, —N(CH$_3$)$_2$), 6.61 (1H, *d*, *J* = 2.4 Hz, Ar—H), 6.81 (1H, *dd*, *J* = 9 Hz, 2.4 Hz, Ar—H), 7.47–7.54 (3H, *m*, Ar—H), 7.66–7.69 (2H, *m*, Ar—H), 7.99 (1H, *s*, H-4), 8.67 (1H, *s*, NH), 9.03 (1H, *s*, NH), 10.92 (1H, *s*, HC=N); ¹³C NMR (DMSO): δ 39.7, 97.1, 108.3, 110.0, 113.2, 113.9, 117.5, 121.6, 129.7, 131.1, 135.2, 138.4, 152.6, 153.2, 155.7, 160.6.

Anal. Calcd for C$_{19}$H$_{17}$BrN$_4$O$_3$ (429.3) C, 53.16; H, 3.99; Br, 18.61; N, 13.05. Found C, 53.18; H, 4.01; Br, ndt; N, 13.07.

(*E*)-1-{[(7-dimethylamino)-2-oxo-2*H*-chromen-3-yl]methylidene}-4-(4-trifluoromethylphenyl)semicarbazone **4**: Obtained from 4-(4-trifluoromethylphenyl)semicarbazide (101 mg) in 98% yield (189 mg), ¹H NMR (DMSO): δ 3.07 (6H, *s*, —N(CH$_3$)$_2$), 6.61
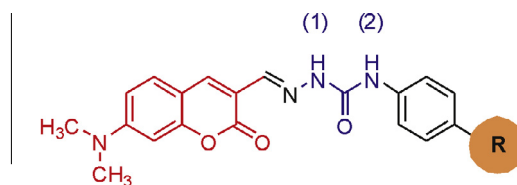
Scheme 1. Molecular structure of the studied molecules.

(1H, *d*, *J* = 2.1 Hz, Ar—H), 6.82 (1H, *dd*, *J* = 8.7 Hz, 2.4 Hz, Ar—H), 7.53 (1H, *d*, *J* = 9 Hz, Ar—H), 7.65 (2H, *d*, *J* = 8.7 Hz, Ar—H), 7.92 (2H, *d*, *J* = 8.4 Hz, Ar—H), 8.02 (1H, *s*, H-4), 8.69 (1H, *s*, NH), 9.26 (1H, *s*, NH), 11.03 (1H, *s*, HC=N); ^{13}C NMR (DMSO): δ 39.7, 97.1, 108.3, 110.0, 113.1, 119.2, 122.4, 125.6, 125.7, 129.8, 135.6, 138.6, 142.8, 152.6, 153.2, 155.8, 160.6.

Anal. Calcd for $C_{20}H_{17}F_3N_4O_3$ (418.4) C, 57.42; H, 4.10; F, 13.62; N, 13.39. Found C, 57.40; H, 4.08; F, ndt; N, 13.38.

(*E*)-1-{[(7-dimethylamino)-2-oxo-2*H*-chromen-3-yl]methyli-dene}-4-(4-cyanophenyl)semicarbazone **5**: Obtained from 4-(4-cyanophenyl)semicarbazide (81 mg) in 98% yield (170 mg), ^{1}H NMR (DMSO): δ 3.07 (6H, *s*, —N(CH_3)_2), 6.61 (1H, *d*, *J* = 2.1 Hz, Ar—H), 6.81 (1H, *dd*, *J* = 8.7 Hz, 2.4 Hz, Ar—H), 7.52 (1H, *d*, *J* = 8.7 Hz, Ar—H) 7.75–7.79 (2H, *m*, Ar—H), 7.90–7.94 (2H, *m*, Ar—H), 8.02 (1H, *s*, H-4), 8.67 (1H, *s*, NH), 9.33 (1H, *s*, NH), 11.08 (1H, *s*, HC=N); ^{13}C NMR (DMSO): δ 39.7, 97.1, 103.8, 108.3, 110.0, 113.0, 119.2, 119.3, 129.8, 132.9, 135.9, 138.7, 143.5, 152.4, 153.2, 155.8, 160.6.

Anal. Calcd for $C_{20}H_{17}N_5O_3$ (375.4) C, 63.99; H, 4.56; N, 18.66. Found C, 63.97; H, 4.54; N, 18.63.

(*E*)-1-{[(7-dimethylamino)-2-oxo-2*H*-chromen-3-yl]methyli-dene}-4-(4-nitrophenyl)semicarbazone **6**: Obtained from 4-(4-nitrophenyl)semicarbazide (90 mg) in 97% yield (177 mg), ^{1}H NMR (DMSO): δ 3.08 (6H, *s*, —N(CH_3)_2), 6.62 (1H, *d*, *J* = 2.4 Hz, Ar—H), 6.82 (1H, *dd*, *J* = 9 Hz, 2.4 Hz, Ar—H), 7.53 (1H, *d*, *J* = 9 Hz, Ar—H) 7.98–8.04 (3H, *m*, Ar—H), 8.21–8.24 (2H, *m*, Ar—H), 8.69 (1H, *s*, NH), 9.53 (1H, *s*, NH), 11.16 (1H, *s*, HC=N); ^{13}C-NMR (DMSO): δ 39.8, 97.2, 108.4, 110.1, 113.1, 118.9, 124.8, 130.0, 136.3, 138.9, 141.5, 145.8, 152.4, 153.4, 155.9, 160.7.

Anal. Calcd for $C_{19}H_{17}N_5O_5$ (394.4) C, 57.72; H, 4.33; N, 17.71. Found C, 57.73; H, 4.35; N, 17.74.

Spectroscopic measurements

Anthracene (zonnally refined 99+ %, Sigma–Aldrich, Germany) was used as the fluorescent standard. The methanol (MeOH), chloroform (CHCl_3), toluene (Tol) and acetonitrile (MeCN) were all UV spectroscopy grade (Scharlau Chemie s.a., Spain).

Polymer films doped with coumarins were prepared by casting from solution. Films of polystyrene (PS) (Chemische Werke Huels, F.R.G.) and poly(methyl methacrylate) (PMMA) (Diacon, ICI, England) were prepared by casting 1 ml chloroform solution of polymer (5 g/100 mL) containing the appropriate amount of probe onto a 28 × 35 mm glass plate. The solvent was evaporated slowly. Films of poly(vinylchloride) (PVC) (Neralit, Spolana Neratovice s.e., CR) were prepared by similar casting from tetrahydrofuran solution. All three polymers were additive free. Remaining solvents were not additionally removed from the polymer.

UV–VIS absorption spectra were recorded by UV 1650PC (Shimadzu, Japan), and fluorescence spectra with a RF-5301PC spectrofluorophotometer (Shimadzu, Japan). The Origin 6.1 (Microcal) was used for data plotting. Solution fluorescence was measured in a 1 cm cuvette in right-angle arrangement and quantum yields were determined relative to anthracene in solution. Polymer film fluorescence was taken in front-face arrangement on the solid sample holder.

The fluorescent quantum yield (Φ_F) of (7-dimethylamino)coumarin *N*-phenylsemicarbazones was determined in solution and in polymer films according to Eq. (1) [33], using anthracene as the standard in the given medium: with a quantum yield of anthracene in cyclohexane of 0.25 [34].

$$\Phi_F = \Phi_F^S \frac{\int_0^\infty I_F(v)dv}{\int_0^\infty I_F^S(v)dv} \left(\frac{A^S}{A}\right) \frac{n^2}{(n^S)^2}, \tag{1}$$

where Φ_F^S is the quantum yield of standard, integrals $\int_0^\infty I_F(v)dv$ and $\int_0^\infty I_F^S(v)dv$ are the areas under the emission curves, A and A^S are absorbances at the excitation wavelength, and n and n^S are refractive indexes of probe and standard solution, respectively. The refractive indexes were considered only for calculation of Φ_F in solution. The anthracene fluorescent quantum yields in the different media were determined by comparison with the anthracene fluorescence in cyclohexane, with values of 0.22 in MeCN, 0.20 in MeOH, 0.11 in CHCl_3 and 0.16 in Tol. The quantum yields in polymer matrices were 0.20 in PMMA, 0.16 in PS and 0.11 in PVC. In this case, the fluorescence of anthracene thin polymer films and standard anthracene solution was measured in the front-face arrangement. The solution and film quantum yields were corrected to different absorptions at the excitation wavelength [33], and fluorescence spectra were taken from excitation at the longest wavelength absorption-band maxima.

The experimental setup for detection of fluorescence lifetimes was based on time-correlated single-photon counting (TCSPC) setup: analogous to that described in detail in [35] (all components from Becker&Hickl GmbH, Berlin, Germany). The procedure is described more simply here: the sample was excited by 375 nm picosecond diode laser with output power ~1 mW, pulse widths typically around 50 ps and frequency rate 20 MHz. The emitted fluorescence was spectrally separated from the laser excitation using 395 nm dichroic filter and 397 nm long-pass filter. A polarizer in magic-angle orientation was fitted in front of the detection system to avoid distortions of decay kinetics due to depolarization effects. The emission was measured by a 16-channel multi-anode photomultiplier array attached to the 160 mm spectrograph (PML-SPEC). The PML detector was run in the photon-counting regime and fed the TCSPC interface card SPC-830. Fluorescence decays were measured in 50 ns time-base, sampled by 1024 temporal channels. The steady-state and time-resolved fluorescence measurements of the coumarinphenylsemicarbazone solutions were performed at 1×10^{-5} mol L^{-1} solute concentrations; except for measurements in Tol, where 3×10^{-6} mol L^{-1} concentration was applied due to limited solubility of some coumarinphenylsemicarbazones in this solvent.

The steady state and time-resolved fluorescence measurements were performed in aerated solutions. All measurements on polymer films were performed in the air.

Theoretical calculations

The relative stability of the coumarinphenylsemicarbazone **6** H-dimers was investigated using quantum-chemical calculations. Structural geometries were optimized at the semiempirical PM6 level. Stationary points were characterized as minima by computations of harmonic vibration frequencies at the same theoretical level as the geometric optimization. Single point energies were calculated at the M062X/6-311++G(d,p) level. All calculations were performed by the Gaussian 09 program package [36].

Results and discussions

Spectral properties

Absorption and emission spectral characteristics of the studied coumarinphenysemicarbazones **1**–**6**, such as the absorption (λ_A) and fluorescence (λ_F) maxima, the molar extinction coefficients (ε), the Stokes shift (v_A–v_F), the fluorescent quantum yield (Φ_F) and the fluorescence lifetime (τ), in various solvents and polymer matrices are presented in Tables 1–3.

Table 1
Spectral data of the studied 3-(7-dimethylamino)coumarin *N*-phenylsemicarbazones **1–6** in Tol at concentration 3×10^{-6} mol L^{-1} and in $CHCl_3$ at concentration 1×10^{-5} mol L^{-1}.

Compd[a] (R)	λ_A[b] (log ε)[c] (nm)	λ_F[d] (nm)	Δv[e] (cm^{-1})	Φ_F[f]	Mean lifetime τ (ns)[g] – χ^2[h]	Results of bi-exponential fitting
Tol						
1 (H)	423 (4.57)	480, 507sh	2752	0.48	1.3 – (1.02)	τ_1 = 0.5 ns (45%)
						τ_2 = 2.1 ns (55%)
2 (F)	421 (4.17)	476, 505sh	2745	0.34	2.3 – (1.12)	τ_1 = 2.1 ns (93%)
						τ_2 = 4.6 ns (7%)
3 (Br)	427 (4.41)	480, 510sh	2586	0.35	1.9 – (1.16)	τ_1 = 1.4 ns (70%)
						τ_2 = 3.1 ns (30%)
4 (CF$_3$)	426 (4.24)	481, 510sh	2684	0.74	1.6 – (1.14)	τ_1 = 1.4 ns (84%)
						τ_2 = 3.2 ns (16%)
5 (CN)	428 (4.66)	482, 510sh	2618	0.46	1.8 – (1.09)	τ_1 = 1.5 ns (88%)
						τ_2 = 3.6 ns (12%)
6 (NO$_2$)	429 (4.23)	481, 510sh	2520	0.57	1.9 – (1.07)	τ_1 = 1.7 ns (86%)
						τ_2 = 3.4 ns (14%)
CHCl$_3$						
1 (H)	433 (4.61)	491, 525sh	2705	0.49	2.7 – (1.13)	τ_1 = 2.3 ns (72%)
						τ_2 = 3.7 ns (28%)
2 (F)	436 (4.63)	478	2015	0.70	3.1 – (1.03)	τ_1 = 2.9 ns (82%)
						τ_2 = 4.1 ns (18%)
3 (Br)	433 (4.60)	491	2728	0.67	3.3 – (1.18)	–
4 (CF$_3$)	433 (4.64)	488, 525sh	2603	0.62	2.7 – (1.18)	τ_1 = 2.3 ns (69%)
						τ_2 = 3.6 ns (31%)
5 (CN)	433 (4.70)	489	2644	0.47	2.7 – (1.13)	τ_1 = 2.4 ns (76%)
						τ_2 = 3.7 ns (24%)
6 (NO$_2$)	436 (4.77)	489	2486	0.16	0.5 – (1.06)	τ_1 = 0.4 ns (95%)
						τ_2 = 2.5 ns (5%)

[a] Structure of the probes according to Scheme 1.
[b] Maximum of main longwavelength absorption band.
[c] Log of the molar extinction coefficient.
[d] Maximum of the fluorescence band and band-shoulder.
[e] Stokes shift.
[f] Quantum yield of fluorescence based on anthracene.
[g] Mean fluorescence lifetime.
[h] Quality of fitting.

Table 2
Spectral data of the studied 3-(7-dimethylamino)coumarin *N*-phenylsemicarbazones **1–6** in MeCN and MeOH at concentration 1×10^{-5} mol L^{-1}.

Compd[a] (R)	λ_A[b] (log ε)[c] (nm)	λ_F[d] (nm)	Δv[e] (cm^{-1})	Φ_F[f]	Mean lifetime τ (ns)[g] – χ^2[h]	Results of bi-exponential fitting
MeCN						
1 (H)	430 (4.59)	503	3375	0.50	2.9 – (1.18)	τ_1 = 2.6 ns (78%)
						τ_2 = 3.9 ns (22%)
2 (F)	424 (4.63)	495	3382	0.37	1.8 – (1.07)	τ_1 = 1.5 ns (87%)
						τ_2 = 3.5 ns (13%)
3 (Br)	429 (4.57)	500	3310	0.92	3.2 – (1.05)	τ_1 = 2.8 ns (88%)
						τ_2 = 5.5 ns (12%)
4 (CF$_3$)	433 (4.25)	499	3055	0.27	2.9 – (1.22)	τ_1 = 2.6 ns (74%)
						τ_2 = 3.7 ns (26%)
5 (CN)	429 (4.62)	500	3310	0.66	2.8 – (1.12)	τ_1 = 2.6 ns (79%)
						τ_2 = 3.8 ns (21%)
6 (NO$_2$)	432 (4.52)	497	3027	0.012	Low intensity	–
MeOH						
1 (H)	431 (4.48)	504	3280	0.64	3.0 – (1.09)	τ_1 = 2.6 ns (67%)
						τ_2 = 3.8 ns (33%)
2 (F)	430 (4.59)	498	3175	0.36	2.5 – (1.10)	τ_1 = 1.8 ns (64%)
						τ_2 = 3.6 ns (36%)
3 (Br)	433 (4.17)	500, 515	3678	~1.00	2.9 – (1.00)	τ_1 = 2.6 ns (79%)
						τ_2 = 4.3 ns (21%)
4 (CF$_3$)	437 (4.48)	500, 515	3466	0.67	2.3 – (1.16)	τ_1 = 1.9 ns (77%)
						τ_2 = 3.6 ns (23%)
5 (CN)	440 (4.57)	499, 518	3422	0.32	2.9 – (1.07)	τ_1 = 2.6 ns (88%)
						τ_2 = 5.2 ns (12%)
6 (NO$_2$)	444 (4.42)	505, 525	3475	0.015	1.5 – (1.06)	τ_1 = 1.3 ns (89%)
						τ_2 = 3.2 ns (11%)

[a] Structure of the probes according to Scheme 1.
[b] Maximum of main longwavelength absorption band.
[c] Log of the molar extinction coefficient.
[d] Maximum of the fluorescence band and band-shoulder.
[e] Stokes shift.
[f] Quantum yield of fluorescence based on anthracene.
[g] Mean fluorescence lifetime.
[h] Quality of fitting.

Table 3
Spectral data of the studied 3-(7-dimethylamino)coumarin *N*-phenylsemicarbazones **1–6** in polymer matrices at concentration 2×10^{-3} mol kg^{-1}.

Compd[a] (R)	λ_A[b] (log ε)[c] (nm)	λ_F[d] (nm)	Δv[e] (cm^{-1})	Φ_F[f]	Mean lifetime τ (ns)[g] – χ^2[h]	Results of bi-exponential fitting
PS						
1 (H)	429 (4.42)	505	3508	0.25	2.6 – (1.10)	–
2 (F)	421 (4.30)	475sh, 510sh, 537	5131	0.15	2.7 – (1.17)	τ_1 = 2.4 ns (76%)
						τ_2 = 4.0 ns (14%)
3 (Br)	432 (4.28)	509, 543	3502	0.12	3.3 – (1.06)	τ_1 = 3.1 ns (89%)
			4732			τ_2 = 5.3 ns (11%)
4 (CF$_3$)	430 (4.38)	475sh, 510sh, 537	4633	0.12	3.0 – (1.06)	τ_1 = 2.6 ns (74%)
						τ_2 = 4.1 ns (26%)
5 (CN)	428 (4.45)	513	3871	0.50	3.2 – (1.32)	τ_1 = 3.0 ns (88%)
						τ_2 = 4.1 ns (12%)
6 (NO$_2$)	432 (3.96)	530	4227	0.13	3.0 – (1.07)	τ_1 = 2.8 ns (78%)
						τ_2 = 3.9 ns (22%)
PVC						
1 (H)	440 (4.43)	505	2925	~1.00	2.3 – (1.10)	–
2 (F)	434 (4.61)	475sh, 555	5023	0.18	3.4 – (1.14)	τ_1 = 3.2 ns (95%)
						τ_2 = 7.5 ns (5%)
3 (Br)	432 (4.79)	508	3463	0.24	3.6 – (1.08)	–
4 (CF$_3$)	439 (4.65)	487sh, 526sh, 547	4498	0.10	3.5 – (1.07)	τ_1 = 2.5 ns (74%)
						τ_2 = 4.2 ns (26%)
5 (CN)	439 (4.52)	512	3248	0.19	4.1 – (1.07)	–
6 (NO$_2$)	442 (4.41)	517	3282	0.17	3.4 – (1.02)	τ_1 = 3.1 ns (75%)
						τ_2 = 4.2 ns (25%)
PMMA						
1 (H)	432 (4.35)	504	3307	~1.00	3.6 – (1.08)	–
2 (F)	425 (4.44)	457sh, 537	4907	0.17	3.2 – (1.13)	τ_1 = 3.0 ns (91%)
						τ_2 = 5.3 ns (9%)
3 (Br)	433 (4.26)	515, 540	3677	0.13	4.0 – (1.09)	–
4 (CF$_3$)	431 (4.50)	515, 532sh	3784	0.31	3.6 – (1.19)	–
5 (CN)	429 (4.48)	517	3968	0.62	4.1 – (1.20)	–
6 (NO$_2$)	432 (4.15)	529	4245	0.48	3.2 – (1.10)	τ_1 = 3.0 ns (76%)
						τ_2 = 4.0 ns (24%)

[a] Structure of the probes according to Scheme 1.
[b] Maximum of main longwavelength absorption band.
[c] Log of the molar extinction coefficient.
[d] Maximum of the fluorescence band and band-shoulder.
[e] Stokes shift.
[f] Quantum yield of fluorescence based on anthracene.
[g] Mean fluorescence lifetime.
[h] Quality of fitting.

Absorption

The absorption spectra of the studied derivatives are quite similar in solution (Figs. S1A–S4A and S8) and in the polymer matrices (Figs. S5A–S7A), exhibiting one intense long-wavelength absorption band without vibrational structure at approximately 430 nm. An exception was noted in derivative **6** spectra where a second absorption band of half-intensity at approximately 330 nm was also present due to the "4-nitroaniline-like" chromophoric system in molecule **6**'s structure.

As expected, the electron-withdrawing ability of the substituent in the *para*-position on the phenyl ring had negligible effect on the λ_A position in the studied fluorophores. The weak effect of *para*-substituent has its origin in intramolecular charge transfer (ICT) during excitation of molecules **1–6**. Electron transition to the locally excited (LE) S$_1$ state is accompanied by electron transfer from a lone electron pair at the nitrogen atom of the dimethylamino group to the coumarin pyranone moiety and exists somewhere between resonance structures I and II depicted in Scheme 2. The electron density change during excitation is localized in the area of the coumarin skeleton and its near neighbourhood. Therefore, the far-distant *para*-substituent (furthermore without the possibility of full π-conjugation effect) does not influence the imine group electron density (partial positive charge on the imine —CH=N— carbon) and thus the λ_A value in most of the solvents.

The negligible effect of the *para*-substituent is also evident in the signal shift for urea moiety -NH- protons in **1–6** ^{1}H NMR spectra (Table S1). Only in the strongly polar protic MeOH solvent, the

λ_A values, particularly those for coumarins **5** and **6** which have the strongest electron-withdrawing substituents (—CN, —NO$_2$) in the *para*-position on the phenyl ring, are shifted more batochromically (~10–15 nm) in comparison with the unsubstituted coumarinphenylsemicarbazone **1** (Table 2). This modest increase in λ_A for coumarins **5** and **6** observed in MeOH is explained by additional stabilization of the ICT character of the LE S$_1$ excited state of coumarinphenylsemicarbazones with strongest electron-withdrawing *para*-substituents by the specific interactions (intermolecular hydrogen bonding) between the coumarinphenylsemicarbazone and corresponding solvent molecules. The LE ICT excited S$_1$ state

1: X = -N-NH-CO-NH-Ph-**H**
2: X = -N-NH-CO-NH-Ph-**F**
3: X = -N-NH-CO-NH-Ph-**Br**
4: X = -N-NH-CO-NH-Ph-**CF3**
5: X = -N-NH-CO-NH-Ph–**CN**
6: X = -N-NH-CO-NH-Ph-**NO2**
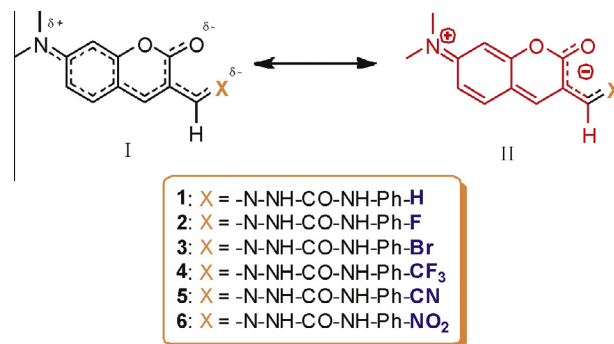
Scheme 2. Charge redistribution in the locally excited singlet S$_1$ states of molecules **1–6** in nonpolar and polar aprotic solvents.
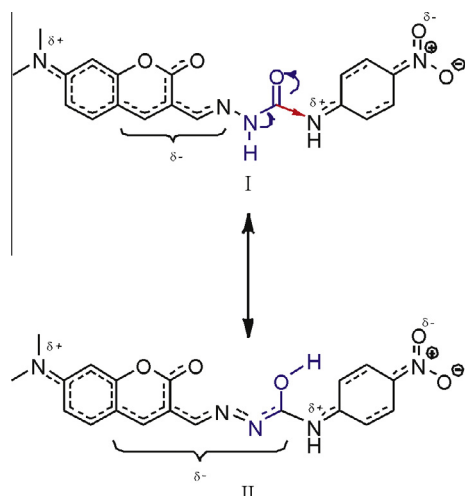
Scheme 3. Presumed charge redistribution in the locally excited singlet S_1 state of molecule **6** in polar protic solvent.

of coumarin **6** depicted in Scheme 3 is shifted slightly to the more conjugated hydrazonol side with deeper ICT character due to the hydrogen bonding stabilization (Scheme 3 – structure II), resulting in decreased S_1 excited state energy, and thus to increased λ_A.

We recently published the concentration and solvent polarity influences on the hydrazide-hydrazonol tautomeric equilibrium of 3-isatin N-phenylsemicarbazone and 3-(N-methyl)isatin N-phenylsemicarbazone E isomers [37].

As expected, the absorption maxima of all derivatives are slightly shifted to longer wavelengths with increasing solvent polarity. The bathochromic shift of λ_A (positive solvatochromism) implies that the electronic transitions corresponding to these bands are $\pi–\pi^*$ transitions. Although deviation of λ_A towards lower energies in the less polar CHCl$_3$ solvent is unexpected compared to MeCN (Tables 1 and 2), halogenated solvents often exert unpredictable effects on solvatochromism of molecules with ICT character [38]. As mentioned in our previous study devoted to unsubstituted coumarinphenylsemicarbazone **1** [27], we assign this effect to decreased stabilization of the ground states of **1–6** by CHCl$_3$ in comparison with other solvents of similar polarity.

Surprisingly, the λ_A values for para-substituted coumarinphenylsemicarabzones **2–6** are slightly red shifted (~10 nm) in PVC compared to the PMMA and PS polymer matrices (Table 3). Similar to the situation in CHCl$_3$, this effect can be connected with decreased stabilization of the ground states of **1–6** by PVC; although, halogen bonding also cannot be excluded.

Emission

Compared to λ_A, the expected stronger dependence of λ_F on solvent polarity and its bathochromic shift with increasing solvent polarity (Tables 1 and 2) accords with additional stabilization of the highly polar LE ICT S_1 state of **1–6** by solvation in polar solvents, typical for 7-(dialkylamino)coumarins [9,12]. Similar to the situation in unsubstituted coumarinphenylsemicarbazone **1**, we assume that the red shift of λ_F for **2–6** (in comparison to the parent 7-(dimethylamino)coumarin-3-carbaldehyde) is associated with rapid additional charge delocalization over the CH=NNHCONHPh moiety in the excited state, as suggested for coumarinphenylsemicarbazone **6** in Scheme 3 – motif II [17]. The additional λ_F shift in polymer matrices (Table 3) most likely caused by coumarinphenylsemicarbazone aggregation in the polymer matrix (see text below). In contrast to symmetrical long-wavelength absorption bands, the fluorescence spectra of derivatives **2–6** often exhibit two overlapping emission bands at approximately 505 (or 485 in

nonpolar solvents) and 540 nm in both solvents and polymer matrices (Figs. S1B–S8B). These two bands changes the ratio of their intensities on moving from one matrix to another. In addition, the fluorescence decay of **2–6** exhibited better fit using the bi-exponential mathematical function (Tables 1–3), although the τ_1 and τ_2 values are quite similar. As observed in the unsubstituted derivative **1** [27], uniform fluorescence excitation spectral shape at these two different emission wavelengths excludes causation by aggregate formation and indicates equilibrium between two emissive ICT excited states. We assume that the origin of the two emissive ICT states for coumarinphenylsemicarbazones **2–6** is connected with the additional charge redistribution in the S_1 state following excitation, and accompanied by the solvent reorganization. This could be further influenced, for example, by equilibrium related to intramolecular hydrogen bond breaking during charge redistribution (Scheme 4).

We recently published the existence of such intramolecular hydrogen bonding in the skeleton of two isatinphenylsemicarbazone derivatives [37,39]. Although the presence of the second isomer can also be responsible for this effect, isomerization of the imine C=N double bond was not observed for derivatives **2–6**.

The Stokes shift of coumarinphenylsemicarbazone varies in the range from 2000 to 5000 cm^{-1}, depending particularly on the ratio of the intensities of two emissive ICT states. Since the increase in $\nu_A–\nu_F$ is associated with the change in the structure of the excited state during its lifetime, one would expect easier reorganization in the solution as in the polymer matrix. Surprisingly, the opposite effect was observed and the largest $\nu_A–\nu_F$ value was recorded for **2** in PS matrix (Table 3).

Compounds **2–6** exhibit high Φ_F in some of the solvents and qualify as laser dyes (k_F higher than k_{nr}) in the given media (Tables 1 and 2). The derivative **3** fluorescent quantum yield approaches 0.92 in MeCN and 1.00 in MeOH. Para-substitution results in increased Φ_F for derivatives **4** and **6** in Tol, for derivatives **2**, **3**, **4** in CHCl$_3$, for **3** and **5** in MeCN, for **3** and **4** in MeOH, and for derivative **5** also in the PS polymer matrix (compared to unsubstituted derivative **1**). Surprisingly, and in sharp contrast to unsubstituted derivative **1** behaviour, para-substitution in polymer matrices leads to relatively rapid decrease in Φ_F value in most para-substituted coumarinphenylsemicarbazones (Table 3); with the only exceptions being high Φ_F values for **5** and **6** in PMMA and increased Φ_F for **5** in the PS matrix. This unexpected decrease in Φ_F values in polymer matrices results from coumarinphenylsemicarbazone-matrix Van der Waals intermolecular interactions and/or coumarinphenylsemicarbazone aggregate formation. The same absorption spectra shape, similar ε values in solutions and polymer matrices and the same shape of the fluorescence excitation spectra at different emission wavelength favours compound-matrix interactions. However, in our previous studies on coumarin fluorescence, we did not observe such considerable quenching effect of all studied polymer matrices on coumarin fluorescence intensity [14,17,40,41]. To the contrary, in most cases the rigidity of the polymer matrix increased coumarin fluorescent quantum yield. Therefore, we assume that the bathochromic shift of λ_F, the largest $\nu_A–\nu_F$ and the lower Φ_F values in the polymer matrix compared to those in solution are from intermolecular interactions in relatively
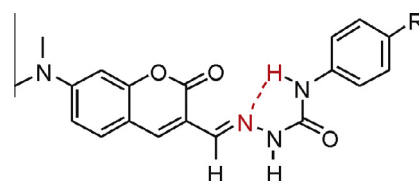
Scheme 4. Intramolecular hydrogen bonding in the structure of the studied coumarinphenylsemicarbazones.
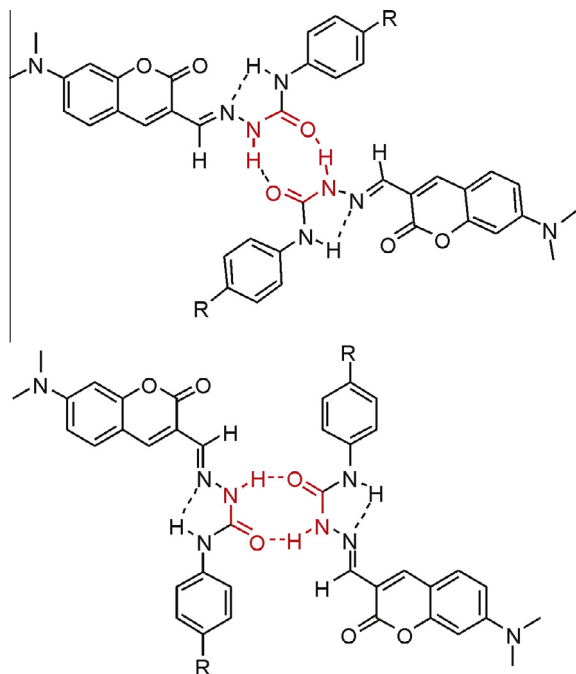
Scheme 5. Possible intermolecular aggregation motifs with negligible influence on the absorption spectra, but which could affect the λ_F position and also significantly support non-radiative deexcitation processes.

high coumarinphenylsemicarbazone concentrations in the polymer matrices (Scheme 5) rather than from coumarinphenylsemicarbazone-matrix interactions. While such intermolecular interactions (originating for example from differing solubility of **2**–**6** compared with that for unsubstituted derivative **1**) have negligible influence on the absorption spectra, they can affect the λ_F position and also significantly support the non-radiative deexcitation processes. The weak fluorescence band shoulders in polymer matrices could also result from this type of aggregation. Further studies should determine which of these processes, or alternate factors, play a key role in these mechanisms.

The fluorescent quantum yield of **6** decreases rapidly with increasing solvent polarity (Tables 1 and 2). We assume the increased solvent polarity most likely leads to population of the highly conjugated non-radiative TICT [42] excited state of **6** (Scheme 6), which results in increase in the non-radiative decay rate constant k_{nr} of the excited S_1 state and thus in gradual Φ_F decrease. The negative charge delocalization and the overall charge separation depicted in Scheme 6 are supported by CT resonance structure stabilization of the "aniline-analogous" end of the molecule 6 skeleton induced by $-M$ mesomeric effect of the $-NO_2$ group.

Solvation in a more polar region results in a decrease in the TICT excited state energy compared to the LE ICT state energy and supports complete electron transfer from the nitrogen atom to the coumarinphenylsemicarbazone residue. The rapid increase in Φ_F
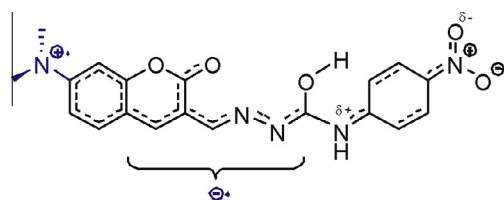
Scheme 6. Proposed charge redistribution in the TICT excited singlet S_1 state of molecule **6**.

of **6** in polar PMMA polymer matrix (Table 3), compared to polar solvents, support this conclusion (PMMA has higher micro-viscosity and decreases the rate of non-radiative deactivation of the S_1 state by rotation suppression). TICT state formation was not observed in unsubstituted derivative **1** nor in other studied *para*-substituted coumarinphenylsemicarbazones, even in highly polar solvents (MeOH, MeCN).

There is controversy in the literature concerning the exact role that hydrogen bonding plays in the formation of the TICT states of 7-aminocoumarins in protic solvents [7,17,43–45]. Recently, Barik et al. published a detailed study with evidence for TICT formation of coumarin C1 only in highly polar protic solvents; and no evidence was supplied for TICT in highly polar aprotic solvents [45]. Similar to the situation in the parent 7-(dimethylamino)coumarin-3-carbaldehyde [27], a rapid decrease in Φ_F for **6** in both MeCN and MeOH (Table 2) and almost equal Φ_F values in these solvents indicate that hydrogen bonding to the solvent is not a necessary condition for TICT stabilization of 7-aminocoumarins in highly polar solvents. Moreover, rapid Φ_F decrease connected with the TICT state formation already in a medium polarity region (CHCl₃; Table 1) supports this finding. As we concluded in our previous paper, the TICT stabilization of 7-aminocoumarins most likely depends on the specific charge redistribution in a particular coumarin, and thus its effect varies from coumarin to coumarin.

To obtain deeper insight into the quenching process of the excited state of **6**, the solvent polarity effect on Φ_F was investigated using the Stern–Volmer relationship (Figs. S9–S12) [46]. As seen in Fig. S9, the stepwise addition of CHCl₃ to the Tol solution of **6** results (rather surprisingly) in fluorescence enhancement up to a CHCl₃ concentration of approximately 2 mol L⁻¹. This unusual Φ_F enhancement at low quencher concentration was also observed after the addition of small amounts of MeCN or MeOH to the Tol solution of **6**. However, the fluorescent enhancement window is narrow and the quenching process starts at lower MeCN or MeOH concentrations than in CHCl₃ addition. Addition of higher quencher concentrations leads to expected fluorescence quenching which complies with typical Stern–Volmer quenching (Figs. S9 and S10). We assume the unusual fluorescence enhancement at low quencher concentrations is connected with stabilization of the CT character of the excited state in more polar solvents, accompanied by an increase in molecule rigidity leading to Φ_F value enhancement. However, further increase in solvent polarity shifts the excited state equilibrium to the non-fluorescent TICT state side resulting in rapid fluorescence quenching in higher concentrations
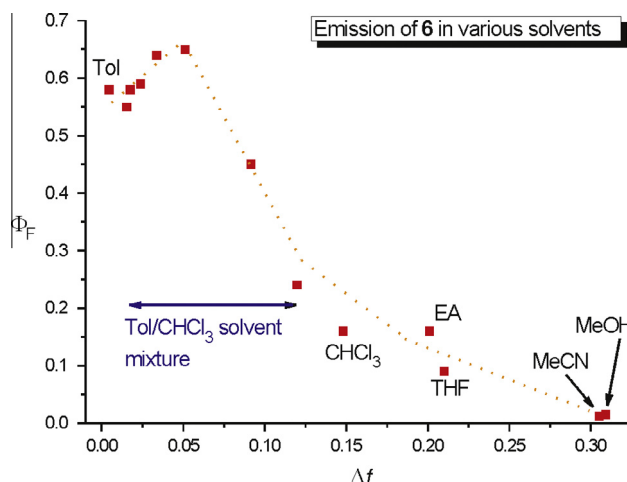
Fig. 1. Fluorescent quantum yield values (Φ_F) for 3-(7-dimethylamino)coumarin *N*-phenylsemicarbazone **6** plotted against solvent polarity factor (Δf): $\lambda_{EX} = \lambda_A$; volume fractions of CHCl₃ in Tol/CHCl₃ solvent mixture were 0.01, 0.02, 0.05, 0.1, 0.2, 0.5 and 0.8.

of a more polar solvent. The unusual exponential decay shape of the $\Phi_F = f(\Delta f)$ curve (Fig. 1) in the medium to high polarity interval is most likely due to TICT state saturation in highly polar solvents.

The quenching process was further investigated using a typical singlet quencher TEMPOL (4-hydroxy-2,2,6,6-tetramethylpiperi-dine-N-oxyl) to confirm the unusual shape of the Stern–Volmer plot at low concentrations of a more polar solvent. In contrast to fluorescence quenching with polar solvents, fluorescence decrease was clearly observed immediately after the initial addition of TEM-POL and it followed the typical Stern–Volmer quenching behaviour (Fig. S10B). Quenching parameters are summarized in Table S2 where bimolecular quenching rate constants (k_q) for MeCN and MeOH are more than one magnitude lower than for TEMPOL. The k_q values for MeCN and MeOH are almost equal and further support our assumption that hydrogen bonding to the solvent is not a necessary condition for TICT stabilization of 7-aminocoumarins in highly polar solvents.

Fig. S10A shows that the Stern–Volmer plot for fluorescence quenching of 6 by MeOH is non-linear at high MeOH concentrations, and accords better with exponential growth function. The non-linearity in the Stern–Volmer plot for 6 at high MeOH concentrations is caused by the ground-state aggregate formation (static quenching) which is discussed in the next section (Self-Aggregation).

Due to the weak intermolecular hydrogen bonding ability of both radiative ICT and non-radiative TICT states, and the steep dependence of Φ_F on solvent polarity, coumarinphenylsemicarbazone 6 appears a useful polarity probe for micro-environments containing hydrogen bonding groups; similar to the parent 7-(dimethylamino)coumarin-3-carbaldehyde [27,47].

Self-Aggregation

The appearance of the new hypsochromically shifted fluorescence excitation band of 6 in MeOH and MeCN (and also for derivatives 4 and 5 in a smaller range), together with apparent concentration dependence of this band at approximately 390 nm, indicates the unusual formation of fluorescent ground-state H-aggregates (Fig. 2, Figs. S13 and S14).

In contrast to the parent 7-(dimethylamino)coumarin-3-carbal-dehyde, aggregate formation was observed in both protic and apro-tic polar solvent, although the presence of the short-wavelength excitation band is similarly more clearly evident in MeOH (Fig. 2). Aggregates of 6 exhibit weaker fluorescence efficiency than the parent carbaldehyde. It is important to note here that the unsubstituted coumarinphenylsemicarbazone 1 exhibits no tendency to fluorescent aggregate formation in protic or aprotic polar solvents [27]. Due to the weaker ICT character of the ground state
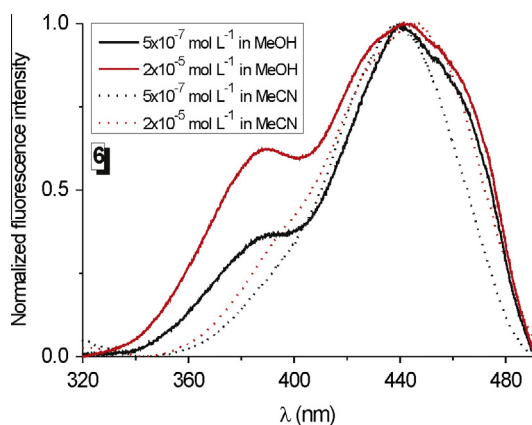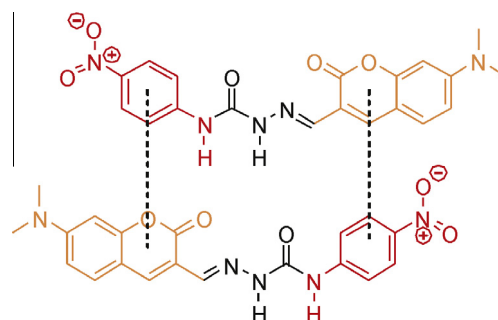
Scheme 7. Possible H-aggregate motif of molecule 6 in highly polar solvents.

of 6 compared to the parent carbaldehyde, we assume that the formation of fluorescent H-dimer aggregates of 6 is driven by dipole–dipole or donor–acceptor π–π interactions between 7-dim-ethylaminocoumarin and *p*-nitroaniline moieties (Schemes 7, S3 and S4), and not by the $\pi(\delta+)$–$\pi(\delta-)$ interactions between two coumarin moieties as occurs in the parent carbaldehyde [27]. Hydrogen bonding interactions between the phenylsemicarbazide chains in such a highly interactive polar solvent as MeOH are precluded. Quantum chemical calculations favour the dipole–dipole dimer formation (Schemes 8 and 9; $\Delta E = 42.4$ kJ mol^{-1} in a vacuum). However, theoretical calculations did not include the dimer-solvent interactions. Therefore, it is difficult to depict the concrete structure of the aggregate at this stage. Unusual H-type aggregate formation of the highly utilized C481 coumarin fluorescent probe in both protic and aprotic polar organic solvents was recently reported by Verma and Pal [48]. Comparison of results from time-resolved emission spectroscopy in EtOH and ACN solutions indicated that, while the polar protic solvent more readily supports C481 dimer formation, the polar aprotic solvent most often leads to the formation of higher aggregates rather than to dimers.

Fluorescence of coumarinphenylsemicarbazone 6 in highly polar solvents is unusual, so care must be taken when interpreting data from fluorescence measurements of 6 at different excitation wavelength in polar environments. On the other side, excitation at the aggregate absorption maximum may help to distinguish between non-interactive and highly interactive polar environments.

Conclusion

In this paper, the spectral properties of five new *para*-phenyl substituted 3-(7-dimethylamino)coumarin *N*-phenylsemicarbaz-ones 2–6 with varying electron-withdrawing substituents in the *para*-position on the phenyl ring were investigated in solution and polymer matrices.

The absorption spectra of the studied derivatives are quite similar in both solution and polymer matrices, exhibiting one intense long-wavelength absorption band without vibrational structure. The electron-withdrawing ability of the substituent in the *para*-position on the phenyl ring has negligible effect on the λ_A position the studied fluorophores.

Compared to λ_A, the expected stronger dependence of λ_F on solvent polarity and its bathochromic shift with increasing solvent polarity is consistent with additional stabilization of the highly polar ICT S_1 state of 2–6 by solvation in polar solvents typical for 7-(dialkylamino)coumarins. The fluorescence spectra of derivatives 2–6 exhibit two overlapping emission bands rather than symmetrical long-wavelength absorption bands. Similarly to the situation in unsubstituted derivative 1, we assume that the origin of two emissive ICT states for coumarinphenylsemicarbazones 2–6 are connected with additional charge redistribution in the S_1 state following excitation, accompanied by the solvent reorganization.

Fig. 2. Excitation spectra of 3-(7-dimethylamino)coumarin *N*-phenylsemicarbaz-one 6 in MeOH and MeCN. Emission wavelength was set at 497 nm.
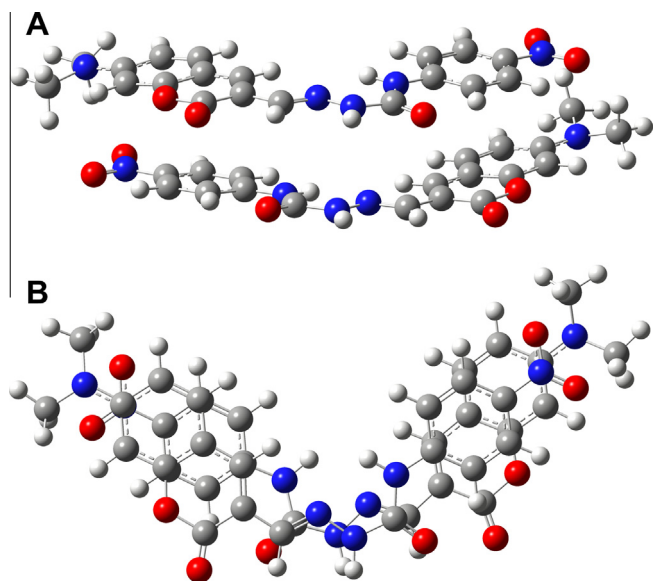
Scheme 8. H-dimer aggregate of **6**, driven by dipole–dipole interactions between 7-dimethylaminocoumarin and *p*-nitroaniline moieties: Optimized geometry found at the PM6 level of theory (A – side view, B – top view); carbon – grey, hydrogen – white, nitrogen – blue, oxygen – red. (For interpretation of the references to colour in this figure legend, the reader is referred to the web version of this article.)
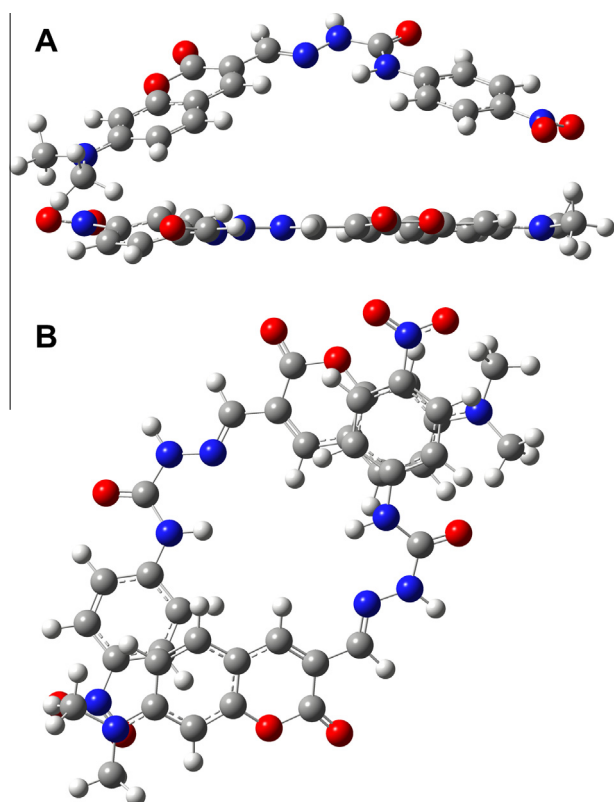
Scheme 9. H-dimer aggregate of **6**, driven by donor–acceptor π–π interactions between 7-dimethylaminocoumarin and *p*-nitroaniline moieties: Optimized geometry found at the PM6 level of theory (A – side view, B – top view); carbon – grey, hydrogen – white, nitrogen – blue, oxygen – red. (For interpretation of the references to colour in this figure legend, the reader is referred to the web version of this article.)

Compounds **2–6** exhibit high Φ_F in some of the solvents, and thus qualify as laser dyes in the given medium, with k_F higher than k_{nr}. For example, the fluorescent quantum yield for derivative **3**

approaches 0.92 in MeCN and 1.00 in MeOH. The *para*-substitution results in increased Φ_F for at least one of the **2–6** derivatives in every type of investigated solvent and also in the PS polymer matrix. In contrast to its effect in solutions, *para*-substitution in polymer matrices quite surprisingly leads to relatively rapid decrease in Φ_F value for most *para*-substituted coumarinphenylsemicarbazones. We assume that this is due to intermolecular interactions in relatively high coumarinphenylsemicarbazone concentrations in the polymer matrix. Although these intermolecular interactions have negligible influence on the absorption spectra, they may affect the λ_F position and also support non-radiative de-excitation processes.

Increased solvent polarity leads to a rapid decrease in Φ_F for NO_2 derivative **6** due to the gradual population of the nonradiative TICT excited state which results in increased nonradiative decay rate constant k_{nr} of the excited state. The rapid decrease in Φ_F for **6** in medium polarity region and almost equal Φ_F values in both protic and aprotic polar solvents indicate that hydrogen bonding to the solvent is not a necessary condition for TICT stabilization of 7-aminocoumarins. As we concluded in our previous paper, the TICT stabilization of 7-aminocoumarins most likely depends on the specific charge redistribution in a particular coumarin, and thus its effect varies from coumarin to coumarin.

Due to the weak intermolecular hydrogen bonding ability of both radiative ICT and non-radiative TICT states, and the steep decrease in Φ_F with increasing solvent polarity, coumarinphenylsemicarbazone **6** appears a useful polarity probe for micro-environments containing hydrogen bonding groups; similar to the parent 7-(dimethylamino)coumarin-3-carbaldehyde.

Contrary to previous reports that many H-aggregates are non-fluorescent in nature, coumarin **6** forms atypical fluorescent H-aggregates in both protic and aprotic polar solvents. Based on previous conclusions valid for the parent 7-(dimethylamino)coumarin-3-carbaldehyde and the unsubstituted coumarinphenylsemicarbazone **1**, we assume that the formation of fluorescent H-dimer aggregates of **6** is driven by dipole–dipole or donor–acceptor π–π interactions between the 7-dimethylaminocoumarin and *p*-nitroaniline moieties. Quantum chemical calculations favour the dipole–dipole dimer formation.

Acknowledgment

Appendix A. Supplementary material

Supplementary data associated with this article can be found, in the online version, at http://dx.doi.org/10.1016/j.saa.2014.01.127.

References

[1] G. Jones II, W.R. Jackson, S. Kanoktanaporn, A.M. Halper, Opt. Commun. 33 (1980) 315–320, http://dx.doi.org/10.1016/0030-4018(80)90252-7.
[2] G. Jones II, W.R. Jackson, C. Choi, W.R. Bergmark, J. Phys. Chem. 89 (1985) 294–300, http://dx.doi.org/10.1021/j100248a024.
[3] A. Nag, K. Bhattacharyya, Chem. Phys. Lett. 169 (1990) 12–16, http://dx.doi.org/10.1016/0009-2614(90)85156-7.
[4] M.S.A. Abdel-Mottaleb, M.S. Antonious, M.M. Abo Ali, L.F.M. Ismail, B.A. El Sayed, A.M.K. Aherief, Proc. Indian Acad. Sci. 104 (1992) 185–196, http://dx.doi.org/10.1007/BF02863363.
[5] R.B. Bangar, T.S. Varandajaran, J. Phys. Chem. 98 (1994) 8903–8905, http://dx.doi.org/10.1021/j100087a014.
[6] S. Nad, H. Pal, J. Phys. Chem. A 105 (2001) 1097–1106, http://dx.doi.org/10.1021/jp003157m.
[7] R. Królicki, W. Jarzęba, M. Mostafavi, I. Lampre, J. Phys. Chem. A 106 (2002) 1708–1713, http://dx.doi.org/10.1021/jp013916g.
[8] S. Nad, M. Kumbhakar, H. Pal, J. Phys. Chem. A 107 (2003) 4808–4816, http://dx.doi.org/10.1021/jp021543t.

[9] P. Dahiya, M. Kumbhakar, T. Mukherjee, H. Pal, Chem. Phys. Lett. 414 (2005) 148–154, http://dx.doi.org/10.1016/j.cplett.2005.08.051.

[10] A.K. Satpati, S. Senthilkumar, M. Kumbhakar, S. Nath, D.K. Maity, H. Pal, Photochem. Photobiol. 81 (2005) 270–278, http://dx.doi.org/10.1111/j.1751-1097.2005.tb00184.x.

[11] U.S. Raikar, C.G. Renuka, Y.F. Nadaf, B.G. Mulimani, A.M. Karguppikar, M.K. Soudagar, Spectrochim. Acta Part A 65 (2006) 673–677, http://dx.doi.org/10.1016/j.saa.2005.12.028.

[12] A.S. Satpati, M. Kumbhakar, S. Nath, H. Pal, Photochem. Photobiol. 85 (2009) 119–129, http://dx.doi.org/10.1111/j.1751-1097.2008.00405.x.

[13] B.D. Wagner, Molecules 14 (2009) 210–237, http://dx.doi.org/10.3390/molecules14010210.

[14] P. Hrdlovič, J. Donovalová, H. Stankovičová, A. Gaplovský, Molecules 15 (2010) 8915–8932, http://dx.doi.org/10.3390/molecules15128915.

[15] M. Danko, E. Szabo, P. Hrdlovič, Dyes Pigments 90 (2011) 129–138, http://dx.doi.org/10.1016/j.dyepig.2010.12.006.

[16] P. Verma, H. Pal, J. Phys. Chem. A 116 (2012) 4473–4484, http://dx.doi.org/10.1021/jp210433f.

[17] J. Donovalová, M. Cigáň, H. Stankovičová, J. Gašpar, M. Danko, A. Gaplovský, P. Hrdlovič, Molecules 17 (2012) 3259–3276, http://dx.doi.org/10.3390/molecules17033259.

[18] M. Cigáň, J. Filo, H. Stankovičová, A. Gaplovský, M. Putala, Spectrochim. Acta Part A 89 (2012) 276–283, http://dx.doi.org/10.1016/j.saa.2012.01.010.

[19] A. Chatterjee, B. Maity, D. Seth, Phys. Chem. Chem. Phys. 15 (2013) 1894–1906, http://dx.doi.org/10.1039/C2CP43483K.

[20] H. Li, L. Cai, Z. Chen, Coumarin-Derived Fluorescent Chemosensors. Advances in Chemical Sensors, Prof. Wen Wang (Ed.), ISBN: 978-953-307-792-5, In Tech, 2012. <http://www.intechopen.com/books/advances-in-chemical-sensors/coumarin-derived-fluorescent-chemosensors>.

[21] A. Prasanna de Silva, H.Q.N. Gunaratante, Th. Gunnlaugsson, A.J.M. Huxley, C.P. Mc, C.P. Mc Coy, J.T. Rademacher, T.E. Rice, Chem. Rev. 97 (1997) 1515–1566, http://dx.doi.org/10.1021/cr960386p.

[22] J. Wu, W. Liu, J. Ge, H. Zhang, P. Wang, Chem. Soc. Rev. 40 (2011) 3483–3495, http://dx.doi.org/10.1039/C0CS00224K.

[23] S. Park, H.-J. Kim, Sens. Actuators B 161 (2012) 317–321, http://dx.doi.org/10.1016/j.snb.2011.10.038.

[24] H. Kwon, K. Lee, H.-J. Kim, Chem. Commun. 47 (2011) 1773–1775, http://dx.doi.org/10.1039/C0CC04092D.

[25] T.-K. Kim, D.-N. Lee, H.-J. Kim, Tetrahedron Lett. 49 (2008) 4879–4881, http://dx.doi.org/10.1016/j.tetlet.2008.06.003.

[26] G.-J. Kim, H.-J. Kim, Tetrahedron Lett. 51 (2010) 4670–4672, http://dx.doi.org/10.1016/j.tetlet.2010.07.003.

[27] M. Cigáň, J. Donovalová, V. Szöcs, J. Gašpar, K. Jakusová, A. Gaplovský, J. Phys. Chem. A 117 (2013) 4870–4883, http://dx.doi.org/10.1021/jp402627a.

[28] J. Shao, Dyes Pigments 87 (2010) 272–276, http://dx.doi.org/10.1016/j.dyepig.2010.04.007.

[29] K. Ghosh, S. Adhikari, Tetrahedron Lett. 47 (2006) 8165–8169, http://dx.doi.org/10.1016/j.tetlet.2006.09.035.

[30] M. Boiocchi, L. Del Boca, D.E. Gómez, L. Fabbrizzi, M. Licchelli, E. Monzani, J. Am. Chem. Soc. 126 (2004) 16507–16514, http://dx.doi.org/10.1021/ja045936c.

[31] R. Flašík, H. Stankovičová, A. Gáplovský, J. Donovalová, Molecules 14 (2009) 4838–4848, http://dx.doi.org/10.3390/molecules14124838.

[32] Y. Liu, K. Cui, W. Lu, W. Luo, J. Wang, J. Huang, C. Guo, Molecules 16 (2011) 4527–4538, http://dx.doi.org/10.3390/molecules16064527.

[33] A. Kawski, A. Kubicki, B. Kuklinski, I. Gryczynski, J. Photochem. Photobiol. A: Chem. 71 (1993) 161–167, http://dx.doi.org/10.1016/1010-6030(93)85068-J.

[34] J.B. Birks, Photophysics of Aromatic Molecules, Wiley-Interscience, London, UK, 1970. pp. 121–127 (Chapter 4).

[35] D. Chorvát, A. Chorvátová, Eur. Biophys. J. 36 (2006) 73–83, http://dx.doi.org/10.1007/s00249-006-0104-4.

[36] M.J. Frisch, G.W. Trucks, H.B. Schlegel, G.E. Scuseria, M.A. Robb, J.R. Cheeseman, G. Scalmani, V. Barone, B. Mennucci, G.A. Petersson, H. Nakatsuji, M. Caricato, X. Li, H.P. Hratchian, A.F. Izmaylov, J.Bloino, G. Zheng, J.L. Sonnenberg, M. Hada, M. Ehara, K. Toyota, R. Fukuda, J. Hasegawa, M. Ishida, T. Nakajima, Y. Honda, O. Kitao, H. Nakai, T. Vreven, J.A. Montgomery Jr., J.E. Peralta, F. Ogliaro, M. Bearpark, J.J. Heyd, E. Brothers, K.N. Kudin, V.N. Staroverov, R.Kobayashi, J. Normand, K. Raghavachari, A. Rendell, J.C. Burant, S.S. Iyengar, J. Tomasi, M. Cossi, N. Rega, N.J. Millam, M. Klene, J.E. Knox, J.B. Cross, V. Bakken, C. Adamo, J. Jaramillo, R. Gomperts, R.E. Stratmann, O. Yazyev, A.J. Austin, R. Cammi, C. Pomelli, J.W. Ochterski, R.L. Martin, K. Morokuma, V.G. Zakrzewski, G.A. Voth, P. Salvador, J.J. Dannenberg, S. Dapprich, A.D. Daniels, Ö. Farkas, J.B. Foresman, J.V. Ortiz, J. Cioslowski, D.J. Fox, Gaussian 09, revision A.1, Gaussian Inc, Wallingford CT, 2009.

[37] K. Jakusová, J. Donovalová, M. Gaplovský, M. Cigáň, H. Stankovičová, A. Gaplovský, J. Phys. Org. Chem. 26 (2013) 805–813, http://dx.doi.org/10.1002/poc.3164.

[38] Y. Ooyama, R. Asada, S. Inoue, K. Komaguchi, I. Imae, Y. Harima, New J. Chem. 33 (2009) 2311–2316, http://dx.doi.org/10.1039/B9NJ00332K.

[39] K. Jakusová, M. Gáplovský, J. Donovalová, M. Cigáň, H. Stankovičová, R. Sokolík, J. Gašpar, A. Gáplovský, Chem. Pap. 67 (2013) 117–126, http://dx.doi.org/10.2478/s11696-012-0248-x.

[40] M. Kaholek, P. Hrdlovič, J. Photochem. Photobiol. A: Chem. 108 (1997) 283–288, http://dx.doi.org/10.1016/S1010-6030(97)00081-6.

[41] M. Kaholek, P. Hrdlovič, J. Bartoš, Polymer 41 (2000) 991–1001, http://dx.doi.org/10.1016/S0032-3861(99)00241-4.

[42] Z.R. Grabowski, K. Rotkiewicz, Chem. Rev. 103 (2003) 3899–4031, http://dx.doi.org/10.1021/cr940745l.

[43] T. López Arbeloa, F. López Arbeloa, M.J. Tapia, I. López Arbeloa, J. Phys. Chem. 97 (1993) 4704–4707, http://dx.doi.org/10.1021/j100120a024.

[44] R.S. Moog, D.D. Kim, J.J. Oberle, S.G. Ostrowski, J. Phys. Chem. A 108 (2004) 9294–9301, http://dx.doi.org/10.1021/jp0486088.

[45] A. Barik, M. Kumbhakar, S. Nath, H. Pal, Chem. Phys. 315 (2005) 277–285, http://dx.doi.org/10.1016/j.chemphys.2005.04.018.

[46] B. Valeur, Molecular Fluorescence: Principles and Applications, Wiley–Verlag CH, GmbH, 2001. pp. 77–79 (Chapter 4).

[47] A. Samanta, R.W. Fessenden, J. Phys. Chem. A 104 (2000) 8972–8975, http://dx.doi.org/10.1021/jp0009960.

[48] P. Verma, H. Pal, J. Phys. Chem. A 117 (2013) 12409–12418, http://dx.doi.org/10.1021/jp409405a.